ChemPubSoc Europe

DOI: 10.1002/chem.201601250

CHEMISTRY A European Journal Full Paper

Polyoxometalates |*Hot Paper*|

The Enhancement on Proton Conductivity of Stable Polyoxometalate-Based Coordination Polymers by the Synergistic Effect of MultiProton Units

Jing Li[+],[a] Xue-Li Cao[+],[b] Yuan-Yuan Wang,[a] Shu-Ran Zhang,[a] Dong-Ying Du,*[a] Jun-Sheng Qin,[a] Shun-Li Li,[a] Zhong-Min Su,*[a] and Ya-Qian Lan*[a, b]

Abstract: Two novel polyoxometalate (POM)-based coordination polymers, namely, $[Co(bpz)(Hbpz)][Co(SO_4)_{0.5}(H_2O)_2(bpz)]_4$ $[PMo^{VI}_8Mo^{V}_4V^{IV}_4O_{42}]\cdot 13H_2O$ (**NENU-530**) and $[Ni_2(bpz)(Hbpz)_3(H_2O)_2][PMo^{VI}_8Mo^{V}_4V^{IV}_4O_{44}]\cdot 8H_2O$ (**NENU-531**) (H_2bpz = 3,3′,5,5′-tetramethyl-4,4′-bipyrazole), were isolated by hydrothermal methods, which represented 3D networks constructed by POM units, the protonated ligand and sulfate group. In contrast with most POM-based coordination polymers, these two compounds exhibit exceptional excellent chemical and thermal stability. More importantly, **NENU-530** shows a high proton conductivity of 1.5×10^{-3} S cm^{-1} at 75 °C and 98% RH, which is one order of magnitude higher than that of **NENU-531**. Furthermore, structural analysis and functional measurement successfully demonstrated that the introduction of sulfate group is favorable for proton conductivity. Herein, the syntheses, crystal structures, proton conductivity, and the relationship between structure and property are presented.

Introduction

The increasing global energy crisis, caused by rapid development of industry and limited natural resources, have accelerated the research in searching for substitute fuels. Among them, proton-exchange membrane fuel cells (PEMFC) as a replacement for traditional engines have attracted remarkable attention due to their high power density and ultralow emission.[1,2] Proton-exchange membrane (PEM) is a vital part of PEMFC.[3] To date, the PEM based on Nafion with high proton conductivity (0.1 S cm^{-1}) is the sole membrane that has been widely used. However, it operates over a low temperature range (< 80 °C) under high relative humidity (98% RH).[4] With the increase in temperature, the conductivity of PEM based on Nafion significantly decreases. Therefore, it is challenging to develop ideal proton-conducting materials operating over a wider temperature range.[5] The amount and mobility of protons as well as the expedite pathway for proton-conducting should be the crucial factors for ideal proton conductors. Furthermore, it is important to explore crystalline proton conductors, which will give insight into the relation between structure and properties in order to further understand the proton-conduction pathway and mechanism.

Polyoxometalates (POMs) are an intriguing class of metal–oxide clusters of nanosize and unique physical and chemical properties.[6] Due to their fascinating structural diversity and oxygen-rich surface with strong coordination ability, POMs show potential applications in catalysis, ion exchange, medicine, gas storage, materials science, and nanotechnology.[7–10] Solid POMs possess a discrete ionic structure, comprising fairly mobile basic structural units, heteropolyanions and counter cations (H^+, H_3O^+, $H_2O_5^+$, etc.). These unique structural features suggest that POMs should exhibit extremely high proton mobility.[2a,11,12] In 1979, Keggin-type POMs ($H_3PMo_{12}O_{40}\cdot 29H_2O$) were first reported as proton conductors by Nakamura and coworkers.[13] Since then, the high proton conduction of POMs has received more attention. Recently, a great number of researchers have focused on the fabrication of POM-based coordination polymers, which are likely to combine the features and functionalities of POMs and coordination polymers or metal–organic frameworks (MOFs) in order to obtain perfect materials with more interesting performances.[14] Firstly, compared to simple MOFs, POM-based coordination polymers show excellent stability and water retention, which are key factors for proton-conducting materials. For instance, Keggin-type POMs can be inlaid into the ordered channels of MOFs, which would endow more hopping sites in the cavities and enhance the stability and hydrophilicity of MOFs. Moreover, polyoxoan-

[a] *Dr. J. Li,[+] Dr. Y.-Y. Wang, Dr. S.-R. Zhang, Dr. D.-Y. Du, Dr. J.-S. Qin, Prof. S.-L. Li, Prof. Z.-M. Su, Prof. Y.-Q. Lan*
Institute of Functional Material Chemistry
Key Laboratory of Polyoxometalate Science of Ministry of Education
Northeast Normal University, Changchun 130024, Jilin (P. R. China)
E-mail: dudy540@nenu.edu.cn
zmsu@nenu.edu.cn

[b] *Dr. X.-L. Cao,[+] Prof. Y.-Q. Lan*
Jiangsu Key Laboratory of Biofunctional Materials
School of Chemistry and Materials Science
Nanjing Normal University, Nanjing 210023, Jiangsu (P. R. China)
E-mail: yqlan@njnu.edu.cn

[+] *These authors contributed equally to this work.*

Supporting information for this article is available on the WWW under http://dx.doi.org/10.1002/chem.201601250.

ions in coordination polymers would be connected with the MOFs by intricate H-bonding networks, which could furnish the pathway for proton conduction. Hence, POM-based coordination polymers might be potentially excellent proton-conductor.

In recent years, network structures, based on phosphonate and sulfonate ligation, have been widely explored in the field of coordination polymers due to their potential functional properties.[15] Strong acids, such as, H_2SO_4 and H_3PO_4, could easily deliver protons along the conduction pathways on account of their strong acidity and low volatility.[16] Hence, phosphate and sulfate groups in the coordination polymer are arguably the favorable candidates for proton conductors. In addition, the introduction of an N-containing ligand is an effective way to enhance proton conductivity. In acid medium, N-containing ligands could be easily charged and would supply mobile protons, which is in favor of proton conduction.

In this study, we take advantage of appropriate N-containing ligands and POMs as well as sulfate groups and have successfully obtained two novel POM-based coordination polymers, namely, $[Co(bpz)(Hbpz)][Co(SO_4)_{0.5}(H_2O)_2(bpz)]_4$-$[PMo^{VI}_8Mo^{V}_4V^{IV}_4O_{42}]\cdot 13\,H_2O$ (**NENU-530**) and $[Ni_2(bpz)$-$(Hbpz)_3(H_2O)_2][PMo^{VI}_8Mo^{V}_4V^{IV}_4O_{44}]\cdot 8\,H_2O$ (**NENU-531**) (H_2bpz = 3,3′,5,5′-tetramethyl-4,4′-bipyrazole). In contrast with most POM-based coordination polymers, these two compounds reveal exceptional chemical and thermal stability. More importantly, **NENU-530** shows a higher proton conductivity of 1.5×10^{-3} S cm^{-1} at 75 °C and 98% RH, which is one order of magnitude higher than that of **NENU-531**. Herein, the syntheses, crystal structures, proton conductivity, and the relationship between structure and property are represented.

Results and Discussion

The X-ray diffraction study demonstrates that **NENU-530** crystallizes in the orthorhombic space group *Fddd* (Table S1 in the Supporting Information). The structure of **NENU-530** features a novel 3D framework based on 2D anionic layers of $[[Co(bpz)(Hbpz)][Co(SO_4)_{0.5}(H_2O)_2(bpz)]_4]^{5-}$ parallel to the *ab*-plane, which are interconnected by the $[PMo^{VI}_8Mo^{V}_4V^{IV}_4O_{42}]^{5+}$ ion clusters. As shown in Figure 1a, its basic structural unit consists of two $[Co(bpz)(Hbpz)]^{-}$ and $[Co(SO_4)_{0.5}(H_2O)_2(bpz)]^{-}$ fragments, $[PMo^{VI}_8Mo^{V}_4V^{IV}_4O_{42}]^{5+}$ ions and thirteen coordination water molecules. There are two crystallographically distinct Co cations. Co(1) adopts a six-coordinated octahedral coordination geometry by two nitrogen atoms from two different bpz ligands, one oxygen atom originating from the $[PMo^{VI}_8Mo^{V}_4V^{IV}_4O_{42}]^{5+}$ cation, one oxygen atom derived from SO_4^{2-} and two coordinated water molecules. Co(2) center also shows an octahedral coordination geometry with four nitrogen atoms from four bpz ligands and two oxygen atoms originating from two different $[PMo^{VI}_8Mo^{V}_4V^{IV}_4O_{42}]^{5+}$ ions. In **NENU-530**, there are two kinds of N-donor ligand, bpz(1) and bpz(2) (Figure S1 in the Supporting Information). One Co(2) cation, four bpz(1) and four Co(1) cations are interlinked into $[Co(bpz)(Hbpz)]^{-}$ and $[Co(SO_4)_{0.5}(H_2O)_2(bpz)]^{-}$ fragments the

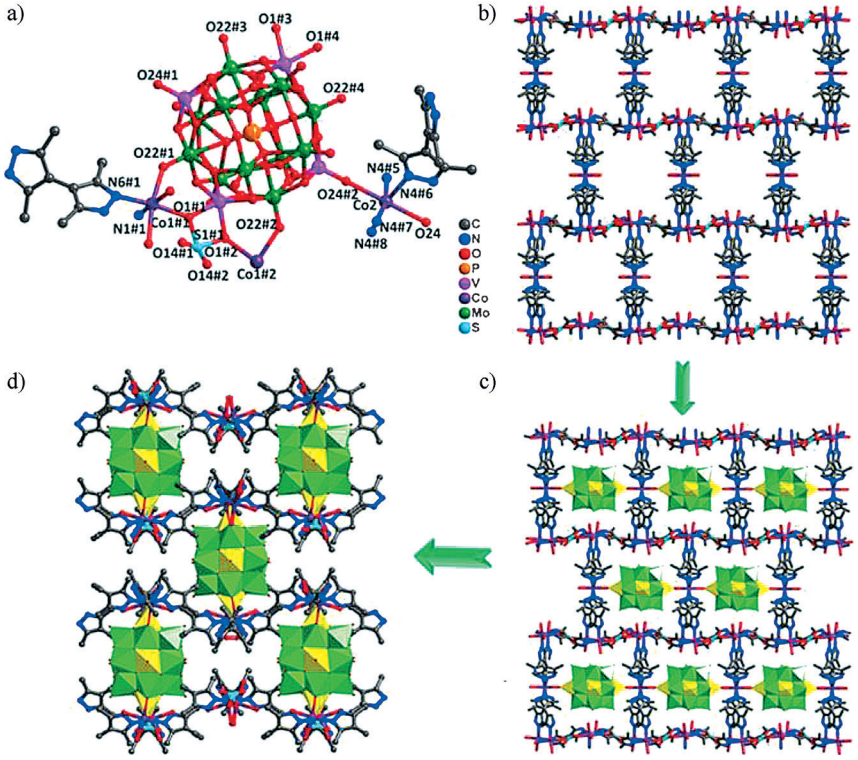

Figure 1. Summary of the structure of **NENU-530**: a) environment of the Co^{II} centers in **NENU-530**. Symmetry code: #1 −1+*x*, *y*, *z*; #2 1.25−*x*, 0.25−*y*, *z*; #3 −1+*x*, 0.25−*y*, 2.25−*z*; #4 1.25−*x*, *y*, 2.25−*z*; #5 −0.25+*x*, 0.5−*y*, 0.25+*z*; #6 1.5−*x*, −0.25+*y*, 0.25+*z*; #7 −0.25+*x*, −0.25+*y*, 2−*z*; #8 1.5−*x*, 0.5−*y*, 2−*z*. b) Ball-and-stick representations of the 2D structure of **NENU-530** along the *c* axis. c) Ball-and-stick representation of the packing arrangement of staggered 2D sheet-like structure in **NENU-530**. d) The 3D framework of **NENU-530**.

$[Co(bpz)(Hbpz)]^-$ fragment, whereas one bpz(2), two Co(1) cations and one SO_4^{2-} group are connected into the $[Co(bpz)(Hbpz)]^-$ fragment. A more interesting feature is that each subunit A (or subunit B) acts as a chelating ligand node, forming left-handed (or right-handed) helical chains in the cationic sheet along the *a* axis (Supporting Information Figure S1). Both left- and right-handed helical chains are linked together via Co(2) cations. Furthermore, a 2D twofold layer is formed by the assembly of these helical chains by sharing two kinds of Z-shaped subunits (Figure 1b and Figure S1 in the Supporting Information). X-ray analysis of **NENU-530** revealed staggered two-dimensional sheets made from Co cluster secondary building units (SBU) bridged by bpz ligands (Figure 1c). Then, each $[PMo^{VI}{}_8Mo^{V}{}_4V^{IV}{}_4O_{42}]^{5+}$ cluster is further linked by staggered two-dimensional sheets to form a 3D framework (Figure 1d and Figure S2 in the Supporting Information). As expected, the $[PMo^{VI}{}_8Mo^{V}{}_4V^{IV}{}_4O_{42}]^{5+}$ ion contains eight Mo^V and four Mo^{VI} ions; the oxidation states of all P and V atoms are +5 and +4, respectively.[17] The overall structure of **NENU-530** is a 3D (3,6,6)-connected network with a Schläfli symbol $\{5\cdot6\cdot7\}_4\{5\cdot6^8\cdot7^2\cdot9^2\cdot10^2\}\{5^4\cdot6^6\cdot7^3\cdot9^2\}$ (Figure S3 in the Supporting Information).

X-ray diffraction analysis shows that **NENU-531** crystallizes in the tetragonal space group P_4/mnc (Table S1 in the Supporting Information). Its structure can be described as a different 3D network composed of 2D layers of $[Ni_2(bpz)(Hbpz)_3(H_2O)_2]^-$ in the *ab*-plane, which are interconnected by $[PMo^{VI}{}_8Mo^{V}{}_4V^{IV}{}_4O_{44}]^+$ cluster. There are one Ni^{II} ion, one bpz ligand, one $[PMo^{VI}{}_8Mo^{V}{}_4V^{IV}{}_4O_{44}]^+$ cation and two coordination water molecules in the basic structural unit (Figure 2a). The unique Ni^{II} cation is in a distorted octahedral geometry composed of four nitrogen atoms from four bpz ligands, one oxygen atom derived from water molecule, and one oxygen atom originated from the $[PMo^{VI}{}_8Mo^{V}{}_4V^{IV}{}_4O_{44}]^+$ ion. The bpz ligands are connected with Ni^{II} ions in the fashion of bridged modes to generate a $(4^4\cdot6^2)$ sheet (Figure 2b). Two neighboring 2D layers are linked by the $[PMo^{VI}{}_8Mo^{V}{}_4V^{IV}{}_4O_{44}]^+$ cationic cluster via Ni–O–V bridges to generate a single 3D porous network with ordered cube-like units of dimensions $13.612\times15.144\times13.612$ Å^3; Figure 2c and d).

The phase purities of **NENU-530** and **NENU-531** were established by comparison of their observed and simulated X-ray powder diffraction (XRPD) patterns (Figure 3), and the IR spectra also indicated their crystalline phase purity (Figure S5 in the Supporting Information). Both compounds are air-stable as no efflorescence of the crystals was observed in air for at least 5 to 8 months. They remained structurally intact after being steeped in common organic solvents (such as dimethylacetamide (DMA), dimethylformamide (DMF), methanol (MeOH), ethanol (EtOH), acetone or dichloromethane) for 3 days at room temperature (Figure 3a and b). Furthermore, they were found to be stable in basic aqueous solution with different pH

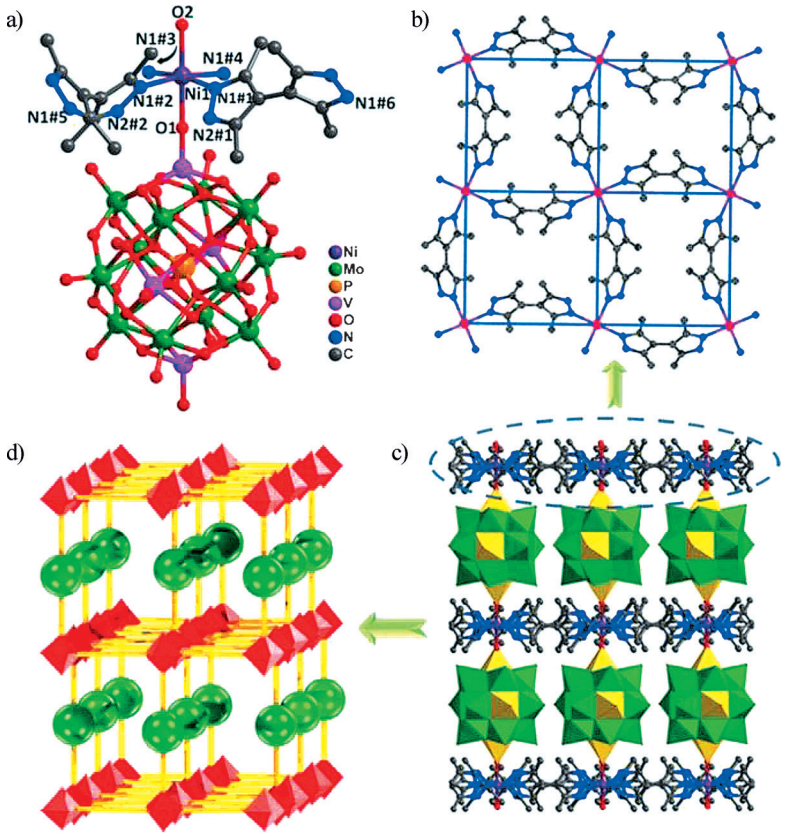

Figure 2. Summary of the structure of **NENU-531**: a) coordination environment of the Co^{II} center. Symmetry code: #1 $-x, y, z$; #2 $-x, -y, z$; #3 $x, -y, z$; #4 0.05599, 0.1418, 0.2532; #5 0.0216, 0.2004, 0.2865; #6 $0.5-x, 0.5+y, 0.5-z$; #7 $0.5-x, 0.5-y, 0.5-z$. b) The 2D layer structure built by Ni^{II} and pbz. c) The 3D framework, and d) ball-stick and polyhedral representations of **NENU-531**.

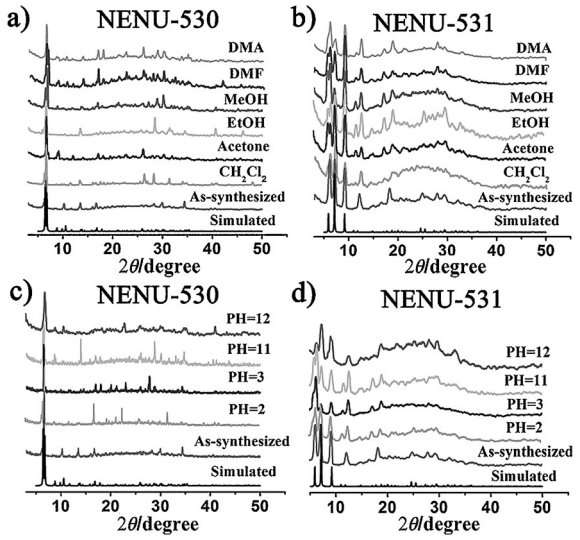

Figure 3. PXRD patterns of the two compounds: a, b) the immersion of **NENU-530** and **NENU-531** in different solvents. c, d) The immersion of **NENU-530** and **NENU-531** in aqueous solutions with different pH values.

values (pH 2, 3, 11, 12; adjusted by HCl or NaOH) at room temperature, as confirmed by the subsequent XRPD patterns (Figure 3c and d). All above-mentioned results reveal that **NENU-530** and **NENU-531** show excellent chemical stability.

To inspect their thermal stabilities, thermogravimetric analysis (TGA) measurements were carried out for **NENU-530** and **NENU-531**. The TGA curve of **NENU-530** reveals that the first step of weight loss of 5.86% (calcd 5.82%) occurred under 400 °C and was attributed to the loss of all lattice water molecules (Figure S6a in the Supporting Information). The second step with the weight loss of 3.43% (400–440 °C) was attributed to the removal of the coordinated water molecules, which matches well with the calculated value of 3.58%. The TGA curve of **NENU-531** shows a continuous weight loss of about 5.8% from room temperature to 380 °C, which is due to the loss of coordinated water molecules and solvent water molecules. The further weight loss above 380 °C may be attributed to the decomposition of the framework (Figure S6b in the Supporting Information). As shown in Figure S7, PXRD patterns for samples heated in flowing N_2 from 100 to 350 °C further confirm that **NENU-530** and **NENU-531** can maintain their crystallinity until 350 °C. Hence, they show excellent thermal and chemical stability which has been reported for few POM-based polymers. This is essential for the broad application of proton conductors.

The vapor adsorption experiments show excellent capacity for water adsorption for both compounds, and the good water retention also favors proton conductivity (Figure S8 in the Supporting Information). The proton conductivity behaviors of both compounds were evaluated by alternating current (AC) impedance spectroscopy with compacted pellets of the powder samples. The bulk conductivity was assessed by semicircle fittings of the Nyquist plots. At 98% RH, the conductivity of **NENU-530** was promoted to 1.5×10^{-3} S cm^{-1} at 75 °C from 2.2×10^{-5} S cm^{-1} at 30 °C (Figure 4c, Table 1 and Table S2 in the Supporting Information). For **NENU-531**, the proton conductivity at 98% RH was improved from 3.8×10^{-6} S cm^{-1} at 30 °C to 1.7×10^{-4} S cm^{-1} at 75 °C (Figure 4c, Table 1 and Table S2 in the Supporting Information), which is one order of magnitude lower than **NENU-530**. More amazingly, the conductivity value of **NENU-530** at 75 °C under 98% RH is one of the best among the conductivity values that have been reported for POM-based coordination polymers (as shown in Table S3 in the Supporting Information).

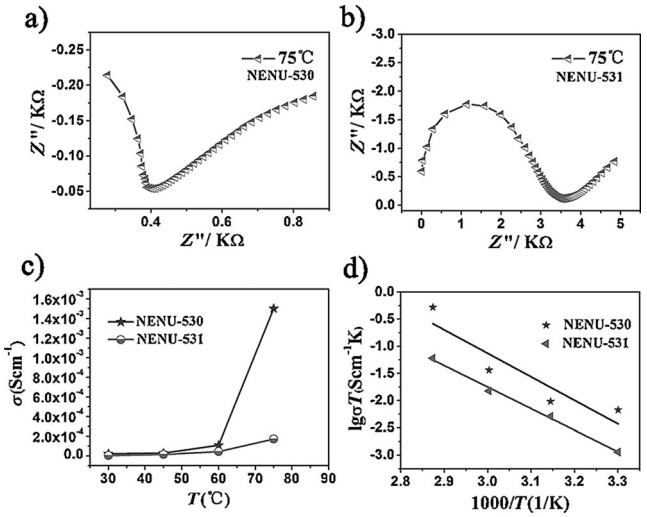

Figure 4. a, b) Nyquist plots of **NENU-530** and **NENU-531** under 75 °C with 98% RH. c) Temperature dependence of the proton conductivity for **NENU-530** and **NENU-531**. d) Arrhenius-type plot of the conductivity of **NENU-530** and **NENU-531** at various temperatures under 98% RH.

Table 1. The factors influencing the proton conductivity of the compounds.

Compound	*T* [K]	σ	Factor
NENU-530	303	2.213E-05	POM; protonated ligand
	333	1.090E-04	sulfate group (SO_4^{2-})
	348	1.503E-03	RH [%]
NENU-531	303	3.745E-06	POM; protonated ligand
	333	4.518E-05	RH [%]
	348	1.733E-04	

However, what is the reason for the high proton conductivity and the significant difference between **NENU-530** and **NENU-531**? Firstly, according to the measurements, the temperature is one of the key factors to improve proton conductivity since the high temperature accelerated proton transition within the channels. Secondly, there are the inseparable relations between crystal structure and high performance: 1) the inlay of the $[PMo_{12}V_4]$ cluster in the framework provided more abundant protons and hopping sites that could speed up transportation in **NENU-530** and **NENU-531**, which further proved that the incorporation of POMs is important for facilitating the internal proton transfer;[18] 2) the protonated H_2bpz and $Hbpz^-$ molecules could provide more protons and this

shows that the ability to form hydrogen bonds contributes to the 3D hydrogen-bonding networks, which is the pathway for proton translocation in both compounds,[19] 3) the presence of sulfate in **NENU-530** should be the crucial factor which results in the significant difference of proton conductivity between these two compounds (Table 1 and Figure S4 in the Supporting Information).

Sulfate groups are extremely significant in various proton conductive polymers just as in Nafion.[20] In **NENU-530**, the strong acid groups ($-SO_4$) could connect with organic ligand and free-water molecules by hydrogen bonds, forming extremely hydrophilic channels and generating well-known advantageous proton-transport pathways, similar to those observed in Nafion. Furthermore, the water sorption isotherms show that the amount of water adsorbed in **NENU-530** is much larger than with **NENU-531**, which might be attributed to the higher hydrophilicity of sulfate groups compared with other groups in the framework (Figure S8). Hence, the presence of sulfate groups should be the key factor that leads to the proton conductivity of **NENU-530** to be one order of magnitude higher than that of **NENU-531** at high humidity.

The temperature dependency of the conductivity was measured, and Arrhenius plots for **NENU-530** and **NENU-531** were obtained as shown in Figure 4d. According to the Arrhenius equation $\sigma T=\sigma_0\exp(-E_a/k_BT)$, the activation energies (E_a) are derived to be 0.33 and 0.36 eV at 98% RH for **NENU-530** and **NENU-531**, respectively, hence the mechanism of proton conductivity should be assigned to the Grotthuss mechanism ($E_a=$ 0.1–0.4 eV).[2a,b,13] This is consistent with the architectural feature that Keggin polyoxoanions are pillared into the channels without mobility. Moreover, as the RH increased from 98 to 75% at 30 °C, the values of proton conductivity for both compounds rose to 2.2×10^{-5} and 3.8×10^{-6} S cm^{-1} from 6.6×10^{-8} and 2.9×10^{-8} S cm^{-1}, respectively (Figures S9 and S10 in the Supporting Information). These prove that RH is a remarkable factor for proton conductivity of both compounds, and further demonstrates that the water absorption of the sample is important in the conduction routes, backing the hypothesis that the proton conduction for both compounds occurs on the basis of the Grotthuss mechanism under water-rich conditions.

Conclusions

In summary, we have designed and synthesized two POM-based coordination frameworks with remarkable thermal and chemical stability by hydrothermal method. The 3D network of **NENU-530** was constructed by POMs, protonated ligands and sulfate groups, three of which could supply acidic protons in **NENU-530**. The excellent proton conductivity of **NENU-530** is as high as 1.5×10^{-3} S cm^{-1} at 75 °C under 98% RH, resulting from the synergistic effect of multiproton units, which is one of the best POM-based materials with one of the highest conductivity values reported in the literature. Compared with **NENU-531**, the proton conductivity of **NENU-530** has been improved distinctly by the introduction of SO_4^{2-} groups in its structure. Our work presents a potential method to enhance the proton conducting properties of hybrid materials by attaching sulfate groups into the polymeric backbones.

Experimental Section

Preparation of NENU-530

A mixture of $H_3PMo_{12}O_{40}\cdot xH_2O$ (0.42 g, 0.23 mmol), NH_4VO_3 (0.44 g, 3.8 mmol), Na_2SO_3 (0.8 g, 6.4 mmol) was dissolved in 7 mL of distilled water at room temperature. The pH was acidified to 5.0 with diluted HCl (2 M). Then, bpz (0.02 g, 0.13 mmol) and $CoCl_2\cdot6H_2O$ (0.2 g, 0.88 mmol) were added to the mixture, which was transferred to and sealed in a 12 mL Teflon-lined stainless steel container, and heated at 120 °C for 3 days. After slow cooling to room temperature, dark blue crystals were filtered and washed with distilled water (43% based on Mo). Elemental analysis (%) calcd for $C_{60}H_{73}Co_5Mo_{12}N_{24}O_{66}PS_2V_4$ (3877.98): C 18.58, H 0.52, Co 7.60, Mo 29.69, N 8.67, P 0.80, S 1.65, V 5.25; found: C 18.47, H 0.63, Co 7.66, Mo 29.53, N 8.78, P 0.78, S 1.70, V 5.33; IR (solid KBr pellet): $\tilde{\nu}=$3324.38 (s), 2924.18 (m), 1620.98 (m), 1559.65 (w), 1537.04 (w), 1455.72 (w), 1419.26 (m), 1373.31 (w), 1281.00 (w), 1145.99 (w), 1030.45 (m), 936.86 (s), 763.00 (s), 654.32 (s), 611.62 (s), 544.28 (m), 490.20 cm^{-1} (m).

Preparation of NENU-531

A mixture of $H_3PMo_{12}O_{40}\cdot xH_2O$ (0.42 g, 0.23 mmol), NH_4VO_3 (0.44 g, 3.8 mmol), Na_2SO_3 (0.8 g, 6.4 mmol) was dissolved in 5 mL of distilled water at room temperature. The pH was acidified to 5.0 with diluted HCl (2 M). Then, bpz (0.016 g, 0.1 mmol) and $NiCl_2\cdot6H_2O$ (0.13 g, 0.80 mmol) were added to the mixture, which was transferred and sealed in a 12 mL Teflon-lined stainless steel container, and heated at 120 °C for 3 days. After slow cooling to room temperature, dark blue crystals were filtered and washed with distilled water (39% based on Mo). Elemental analysis (%) calcd for $C_{40}H_{51}Mo_{12}N_{24}Ni_2O_{54}PV_4$ (3232.58): C 14.86, H 1.50, Ni 3.63, Mo 35.62, N 10.40, P 0.96, V 6.30; found: C 14.75, H 1.58, Ni 3.50, Mo 35.78, N 10.34, P 0.92, V 6.44. IR (solid KBr pellet): $\tilde{\nu}=$3219.14 (m), 1617.84 (m), 1556.84 (w), 1420.36 (m), 1372.29 (w), 1284.17 (w), 1251.51 (w), 1159.33 (w), 1062.79 (m), 1033.00 (m), 949.25 (s), 877.16 (s), 792.90 (s), 655.04 (s), 535.52 cm^{-1} (s).

CCDC 1449386 (**NENU-530**) and 1449387 (**NENU-531**) contain the supplementary crystallographic data for this paper. These data are provided free of charge by The Cambridge Crystallographic Data Centre.

Acknowledgements

This work was financially supported by the National Natural Science Foundation of China (No. 21371099, 21401021 and 21471080), China Postdoctoral Science Foundation (No. 2015T80284), NSF of Jiangsu Province of China (No. BK20130043 and BK20141445), Priority Academic Program Development of Jiangsu Higher Education Institutions, and Foundation of Jiangsu Collaborative Innovation Center of Biomedical Functional Materials.

Keywords: coordination chemistry · coordination polymers · polyoxometalates · proton conductivity · sulfate

[1] a) R. F. Service, *Science* **2002**, *296*, 1222 – 1224; b) K. D. Kreuer, S. J. Paddison, E. Spohr, M. Schuster, *Chem. Rev.* **2004**, *104*, 4637 – 4678; c) H. Zhang, P. K. Shen, *Chem. Rev.* **2012**, *112*, 2780 – 2832; d) S. J. Peighambardoust, S. Rowshanzamir, M. Amjadi, *Int. J. Hydrogen Energy* **2010**, *35*, 9349 – 9384; e) M. Yoon, K. Suh, H. Kim, Y. Kim, N. Selvampalam, K. Kim, *Angew. Chem. Int. Ed.* **2011**, *50*, 7870 – 7873; *Angew. Chem.* **2011**, *123*, 8016 – 8019; f) C. Laberty-Robert, K. Valle, F. Pereira, C. Sanchez, *Chem. Soc. Rev.* **2011**, *40*, 961 – 1005; g) P. Tölle, C. Köhler, R. Marschall, M. Sharifi, M. Wark, T. Frauenheim, *Chem. Soc. Rev.* **2012**, *41*, 5143 – 5159; h) J. C. McKeen, Y. S. Yan, M. E. Davis, *Chem. Mater.* **2008**, *20*, 3791 – 3793; i) D. Basak, C. Versek, D. T. Toscano, S. Christensen, M. T. Touminen, D. Venkataraman, *Chem. Commun.* **2012**, *48*, 5922 – 5924.

[2] a) M. Yoon, K. Suh, S. Natarajan, K. Kim, *Angew. Chem. Int. Ed.* **2013**, *52*, 2688 – 2700; *Angew. Chem.* **2013**, *125*, 2752 – 2764; b) T. Yamada, K. Otsubo, R. Makiura, H. Kitagawa, *Chem. Soc. Rev.* **2013**, *42*, 6655 – 6669; c) S. L. Li, Q. Xu, *Energy Environ. Sci.* **2013**, *6*, 1656 – 1683.

[3] a) D. K. Kreuer, *Chem. Mater.* **1996**, *8*, 610 – 641; b) G. Alberti, U. Costantino, M. Casciola, S. Ferroni, L. Massinelli, P. Staiti, *Solid State Ionics* **2001**, *145*, 249 – 255.

[4] Q. Li, R. He, J. O. Jensen, N. J. Bjerrum, *Chem. Mater.* **2003**, *15*, 4896 – 4915.

[5] a) M. Yamada, D. Li, I. Honma, H. Zhou, *J. Am. Chem. Soc.* **2005**, *127*, 13092 – 13093; b) M. T. Colomer, *Adv. Mater.* **2006**, *18*, 371 – 374; c) S. Fujita, A. Koiwai, M. Kawasumi, S. Inagaki, *Chem. Mater.* **2013**, *25*, 1584 – 1591.

[6] a) M. T. Pope, A. Müller, *Angew. Chem. Int. Ed. Engl.* **1991**, *30*, 34 – 48; *Angew. Chem.* **1991**, *103*, 56 – 70; b) L. Cronin, A. Müller, *Chem. Soc. Rev.* **2012**, *41*, 7333 – 7334; c) H. N. Miras, J. Yan, D. L. Long, L. Cronin, *Chem. Soc. Rev.* **2012**, *41*, 7403 – 7430; d) A. Banerjee, B. S. Bassil, G. V. Roschenthaler, U. Kortz, *Chem. Soc. Rev.* **2012**, *41*, 7590 – 7604.

[7] H. Lv, Y. V. Geletii, C. Zhao, J. W. Vickers, G. Zhu, Z. Luo, J. Song, T. Lian, D. G. Musaev, C. L. Hill, *Chem. Soc. Rev.* **2012**, *41*, 7572 – 7589.

[8] J. T. Rhule, C. L. Hill, D. A. Judd, R. F. Schinazi, *Chem. Rev.* **1998**, *98*, 327 – 358.

[9] J. M. Clemente-Juan, E. Coronado, A. Gaita-Arino, *Chem. Soc. Rev.* **2012**, *41*, 7464 – 7478.

[10] Y. Wang, I. A. Weinstock, *Chem. Soc. Rev.* **2012**, *41*, 7479.

[11] D. E. Katsoulis, *Chem. Rev.* **1998**, *98*, 359 – 388.

[12] I. V. Kozhevnikov, *Chem. Rev.* **1998**, *98*, 171 – 198.

[13] O. Nakamura, T. Kodama, I. Ogino, Y. Miyake, *Chem. Lett.* **1979**, *8*, 17 – 18.

[14] a) D. Y. Du, J. S. Qin, S. L. Li, Z. M. Su, Y. Q. Lan, *Chem. Soc. Rev.* **2014**, *43*, 4615 – 4632; b) Q. Han, X. Sun, J. Li, P. Ma, J. Niu, *Inorg. Chem.* **2014**, *53*, 6107 – 6112; c) B. Nohra, H. El Moll, L. M. Rodriguez Albelo, P. Mialane, J. Marrot, C. Mellot-Draznieks, M. O'Keeffe, R. Ngo Biboum, J. Lemaire, B. Keita, L. Nadjo, A. Dolbecq, *J. Am. Chem. Soc.* **2011**, *133*, 13363 – 13374.

[15] G. K. H. Shimizu, R. Vaidhyanathan, J. M. Taylor, *Chem. Soc. Rev.* **2009**, *38*, 1430 – 1449.

[16] a) M. F. H. Schuster, W. H. Meyer, *Annu. Rev. Mater. Res.* **2003**, *33*, 233 – 261; b) T. Tezuka, K. Tadanaga, A. Hayashi, M. Tatsumisago, *J. Am. Chem. Soc.* **2006**, *128*, 16470 – 16471.

[17] C. M. Liu, D. Q. Zhang, D. B. Zhu, *Cryst. Growth Des.* **2006**, *6*, 524 – 529.

[18] Y. W. Liu, X. Yang, J. Miao, Q. Tang, S. M. Liu, Z. Shi, S. X. Liu, *Chem. Commun.* **2014**, *50*, 10023 – 10026.

[19] M. L. Wei, X. X. Wang, X. Y. Duan, *Chem. Eur. J.* **2013**, *19*, 1607 – 1616.

[20] a) X. Y. Dong, R. Wang, J. Z. Wang, S. Q. Zang, T. C. W. Mak, *J. Mater. Chem. A* **2015**, *3*, 641 – 647; b) W. J. Phang, H. Jo, W. R. Lee, J. H. Song, K. Yoo, B. S. Kim, C. S. Hong, *Angew. Chem. Int. Ed.* **2015**, *54*, 5142 – 5146; *Angew. Chem.* **2015**, *127*, 5231 – 5235.

Received: March 16, 2016
Published online on May 31, 2016